Medium Voltage Three-level Converters for the Grid Connection of a Multi-MW Wind Turbine

Osman S. Senturk[1] Lars Helle[2] Stig Munk-Nielsen[1] Pedro Rodriguez[3] Remus Teodorescu[1]
[1]AALBORG UNIVERSITY [2]VESTAS WIND SYSTEMS [3]TECH. UNI. OF CATALONIA
Pontoppidanstraede 101
Aalborg, Denmark
Tel.: +45 / (0) – 9940 9283
Fax: +45 / (0) – 9815 1411
E-Mail: oss@iet.aau.dk
URL: http://www.iet.aau.dk

Acknowledgements

This work was supported by Aalborg University-Vestas Wind Systems partnership under Vestas Power Program. Any opinions, findings, and conclusions or recommendations expressed in this material are those of the authors and do not necessarily reflect those of Vestas Wind Systems.

Keywords

«Multilevel converters», «Wind energy»

Abstract

Three-level (3L) neutral point clamped (NPC), flying capacitor (FC), and H-bridge (HB) voltage source converters (VSCs) as a grid-side full-scale medium voltage (MV) converter are modeled, controlled, and simulated for the grid connection of a hypothetical 6MW wind turbine. Via the converter topological features and the simulation results demonstrating the converter performance, these three 3L-VSCs are discussed and compared in terms of power density and reliability, which can be considered as two of the most important criteria for the converters placed in wind turbine nacelles. Given the grid connection circuit (without capacitive switching ripple filters), the 3L-HB-VSC is expected to be superior with respect to power density and reliability over the 3L-NPC- and -FC-VSCs.

Introduction

Globally, cumulative wind power installed capacity has reached around 120GW and it has been forecasted that this capacity will be tripled by the end of the next 5-year period between 2008 and 2013 [1]. In this development, the increasing contribution of multi-MW (>2.5MW) wind turbines can be expected considering that their annual market share has already developed significantly from 4.3% (688MW) in 2006 to 6.0% (1877MW) in 2008 [1]. In the multi-MW wind turbine market, the maximum power rating of a commercial wind turbine has reached 6MW [1] by the concern of generating more power from wind power sites. However, the interface between wind turbine and electricity grid in order to penetrate MWs of wind power in accordance with grid codes is another important concern regarding that the grid codes regulating this penetration are getting stricter [2]. Therefore, full-scale power electronic converters, which process all wind turbine output power to ensure compliance with these grid codes, are attracting interest in wind power generation technology. Mainly, there are two full-scale converter options: single unit of a medium voltage (MV) converter [3] and parallel units of low voltage (LV) converters [4]. These two solutions could be compared and discussed in terms of power density, reliability, complexity, modularity, converter topology, supported turbine technology, and cost. However, to be able to do so fairly, detailed research studies should be conducted beforehand in this area, where the literature and the technology are now under a fast development. As a contribution to this growing literature, this study will investigate several MV

converter solutions considering their grid-side power quality performance and switch utilization under normal conditions.

Power electronic converters in MV are generally realized as multi-level (ML) voltage source converters (VSC) instead of 2L-VSCs in order to improve the figures of switch power losses, harmonic distortion, dv/dt, and common mode voltage/current [5]. In the literature, there are three main ML-VSC topologies, which are neutral point clamped (NPC) [6], flying capacitor (FC) [7], and cascaded H-bridge (CHB) [8]. For MV AC drive applications, these topologies have been studied in the literature extensively [5], [9] and compared in detail [10]. Also, these topologies have been employed in the MV AC drive market successfully. However, they have not been elaborately studied, extensively applied, and fairly compared for the wind turbine applications despite there are several studies such as [3], [11], [12].

This study considers the interface of a hypothetical 6MW wind turbine with 10kV grid via 3L-NPC, -FC-, and -HB-VSCs with 4.5kV press-pack IGBT-diode pairs. The VSCs are modeled, controlled, and simulated in such detail that these VSCs' performance is demonstrated comparatively in terms of converter output current total harmonic distortion (THD_I), switch power losses, and power loss distribution. This effort along with the consideration of each VSC's topological features aims to give an insight about the power density and reliability of these three VSCs as a grid interface circuitry to be built in a nacelle. Given the grid connection circuit (without capacitive switching ripple filters like LCL filter), the 3L-HB-VSC is anticipated to be superior in terms of power density and reliability over the 3L-NPC- and -FC-VSCs.

In this paper, first, the 3L NPC, FC, and HB topologies, their modulations, and their controls are briefly explained. Secondly, the wind turbine grid connection including grid, step-up transformer, 3L-VSCs, and the IGBT-diode pairs, is modeled in sufficient detail. Next, the simulation results comprising of output voltage/current waveforms, converter output current harmonic spectrums, switch current waveforms, and switch power losses are represented. Finally, these three VSCs are discussed and compared with respect to power density and reliability.

Three-level Medium Voltage Converter Topologies and Their Controls

3L-NPC-, -FC-, and -HB-VSCs shown in Fig. 1-3 are able to produce three levels of voltages such as V_{DC}, 0, and $-V_{DC}$ per phase by making use of neutral point clamps, flying capacitors, and two-2L legs, respectively. Opposed to the other two converters, the 3L-HB-VSC requires open-winding (at converter side) transformer or independent DC buses in order not to cause any undesired current circulation among the three HBs. It should be noted that the DC bus voltages of the NPC and FC converters are $2V_{DC}$ whereas the DC bus voltages of the HB converter and the flying capacitor voltages of the FC converter are V_{DC}.

The power flow via each VSC power circuit is controlled via an identical closed-loop current controller (realized in dq frame), which takes the reference current corresponding to the real and reactive powers to be delivered to the grid and produces the reference voltages. Then, the modulation signals for IGBT switches corresponding to the reference output voltages are produced by space vector pulse-width modulation (SVPWM) with near three vector (NTV) approach such that each VSC can produce the same output voltages for the same reference voltages [13]-[15]. However, neutral point and flying capacitor voltage balance controls, which have slight effects on the converter performance at steady-state, are considered to be beyond the scope of this study and not included.

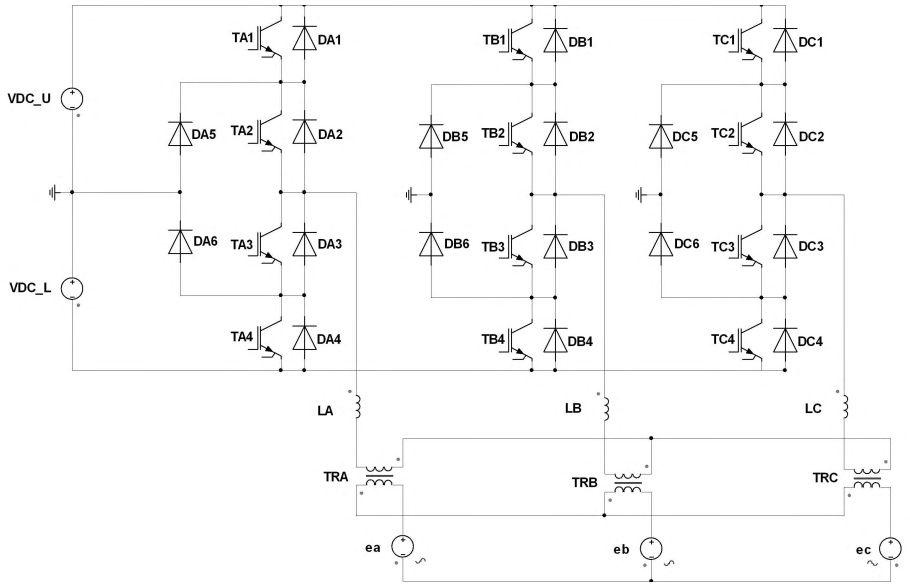

Fig. 1: Wind turbine grid connection via a 3L-NPC-VSC

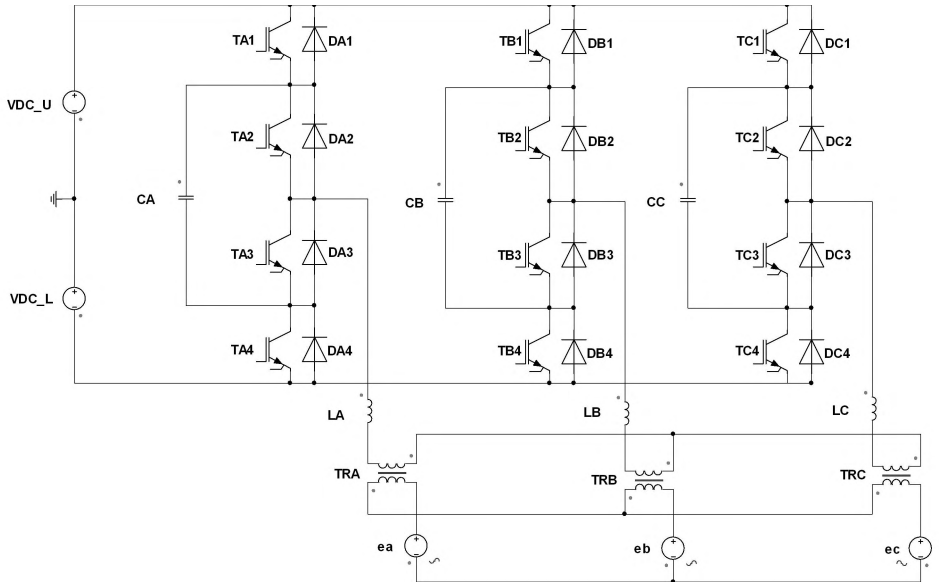

Fig. 2: Wind turbine grid connection via a 3L-FC-VSC

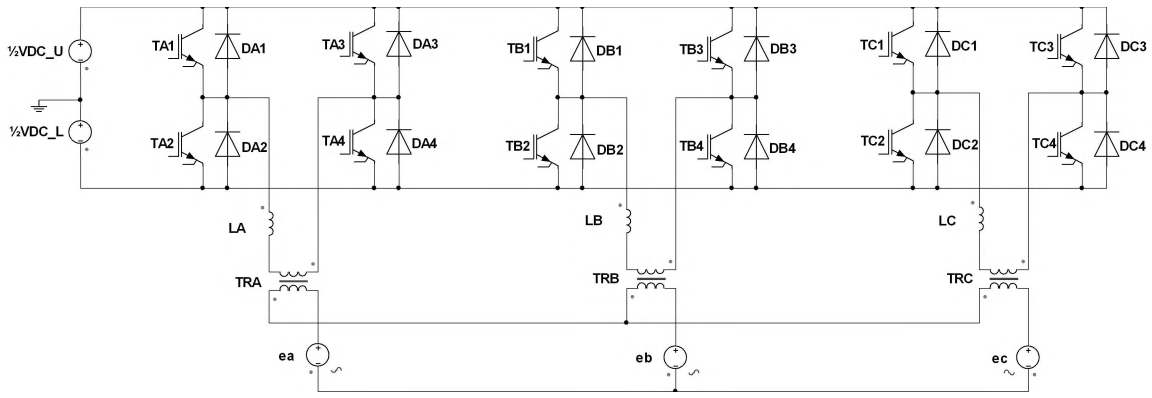

Fig. 3: Wind turbine grid connection via a 3L-HB-VSC

Modeling of the Wind Turbine Grid Connection

The grid connection of the wind turbine is modeled by ideal DC voltage sources, converters with ideal IGBTs and diodes, infinitely large flying capacitors, 10% filter inductors, ideal step-up transformers, and 10kV grid. The parameters of the simulation model are given in Table I. The limits for PF and f_S are selected considering grid code requirements and MV switch capabilities, respectively. Moreover, the turn-on, turn-off/recovery, and conduction power losses of IGBTs and diodes are modeled as look-up tables by means of the utilization of turn-on energy (E_{on} vs. V_{CE} and I_C), turn-off energy (E_{off} vs. V_{CE} and I_C), reverse recovery energy (E_{rec} vs. V_D and I_D), and on-state voltage drop ($V_{CE,sat}$ vs. I_C and $V_{D,on}$ vs. I_D) curves given in the datasheet of a 4.5kV-1.8kA Westcode press-pack IGBT-diode pair (T1800GA45A) [16]. It should be noted that the turn-on losses of diodes are neglected [17].

Table I: Model parameters for the wind turbine grid connection with the 3L-VSCs

Model	Symbol	Quantity	Value
Electricity Grid	$V_{S,LL}$	Line-to-line voltage (50Hz)	10kV
	PF	Power factor	1-0.9 (ind.)
Turbine	P	Rated power	6MW
Converter	V_{DC}	DC bus voltage	2500V
	$V_{C,LL}$	Output line-to-line voltage	3kV
	f_S	Switching frequency	650-1050Hz
	L	Filter inductance	450µH (10%)
Transformer	N_{TR}	Transformer turns ratio (N_{grid}:N_{conv})	3.33

Simulation Results

The 6MW wind turbine grid connection models for the 3L-NPC-, -FC-, and -HB-VSCs are simulated via Ansoft-Simplorer under the four cases of f_S=1050Hz & PF=1, f_S=1050Hz & PF=0.9, f_S=650Hz & PF=1, and f_S=650Hz & PF=0.9. Given in Fig. 4, voltage/current waveforms and current harmonic spectrums for the case of f_S=1050Hz & PF=1 show that each converter produces the identical outputs with THD_I of 8.9% despite there is negligible discrepancy (around 0.1%) at several harmonic frequencies. For the case of f_S=1050Hz & PF=0.9, Fig. 5 demonstrates that the identical output performance of the three converters (THD_I=8.3%). For the cases of f_S=650Hz & PF=1 and f_S=650Hz & PF=0.9, Fig. 6 shows the output voltage and current waveforms of the converters, where THD_I values are 14.3% and 13.3%, respectively. Table II summarizes THD_I for all the cases.

Switch utilization of each converter for the case of f_S=1050Hz & PF=1 is illustrated in Fig. 7 by means of the IGBT and diode current waveforms for phase-a. As seen in the figure, the outer IGBTs of the NPC (TA1 and TA4) do switch twice the IGBTs of the FC and HB while the inner IGBTs of the NPC (TA2 and TA3) do not switch at all. Similarly, the clamping diodes (DA5 and DA6) switch twice the antiparallel diodes of the FC and HB whereas the antiparallel diodes of the NPC are almost idle. In Fig. 8, the switch utilization in these converters can also be seen via the charts representing the power losses of turn-on (P_{on}), turn-off/recovery (P_{off}/P_{rec}), and conduction (P_{con}) of each IGBT and each diode. The figure shows that at least 50% of the total power loss (P_{loss}) is comprised of P_{con}, which is independent from f_S unlike P_{on}, P_{off}, and P_{rec}. Also, the figure demonstrates that the switch utilization is not significantly influenced by the PF decrease from 1 to 0.9. Table II summarizes P_{loss} for all the cases and shows that P_{loss} values for the three VSCs under a specific case are almost equal.

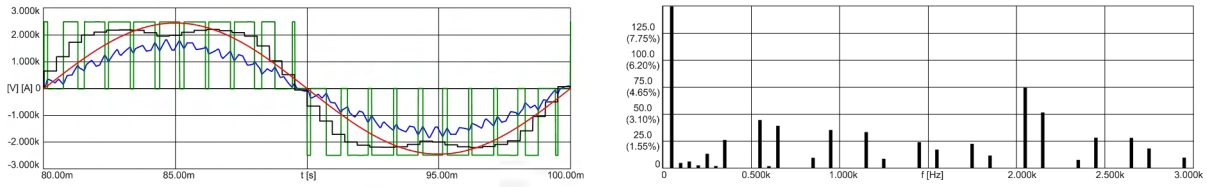

(a) NPC

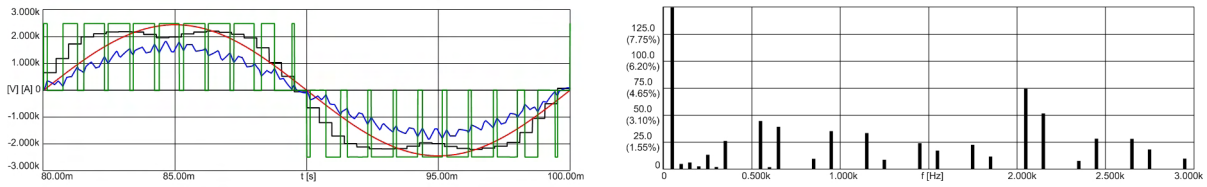

(b) FC

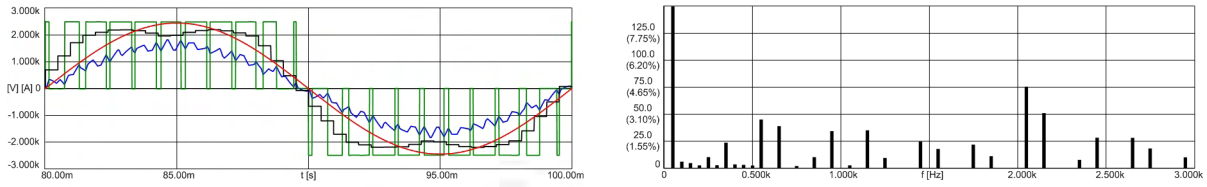

(c) HB

Fig. 4: For f_S=1050Hz & PF=1; (LEFT) the grid voltage (red, scaled by N_{TR}^{-1}=0.3), the converter output voltage (green), the converter reference voltage (black), and the converter output current (blue) for phase-a of each VSC; (RIGHT) the converter output current harmonic spectrums for phase-a of the VSCs

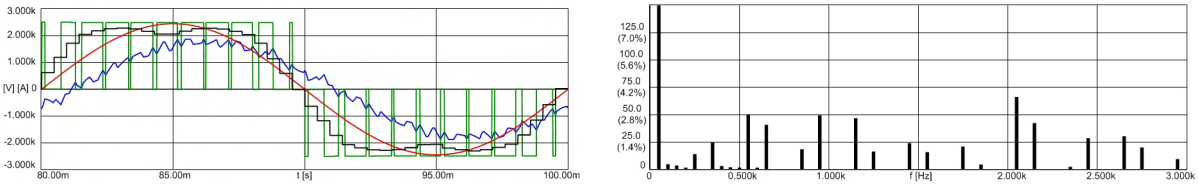

Fig. 5: For f_S=1050Hz & PF=0.9; (LEFT) the grid voltage (red, scaled by N_{TR}^{-1}=0.3), the converter output voltage (green), the converter reference voltage (black), and the converter output current (blue) for phase-a of the VSCs; (RIGHT) the converter output current harmonic spectrums for phase-a of the VSCs

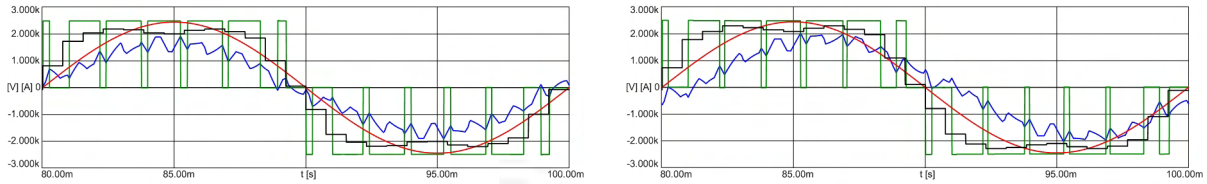

(a) f_S=650Hz & PF=1 (b) f_S=650Hz & PF=0.9

Fig. 6: For f_S=650Hz, the grid voltage (red, scaled by N_{TR}^{-1}=0.3), the converter output voltage (green), the converter reference voltage (black), and the converter output current (blue) for phase-a of the VSCs

Table II: THD_I and P_{loss} of the 3L-VSCs

	NPC				FC				HB			
	f_S=1050Hz		f_S=650Hz		f_S=1050Hz		f_S=650Hz		f_S=1050Hz		f_S=650Hz	
	PF =1	PF =0.9	PF =1	PF =0.9	PF =1	PF =0.9	PF =1	PF =0.9	PF =1	PF =0.9	PF =1	PF =0.9
THD_I (%)	8.9	8.3	14.3	13.3	8.9	8.3	14.3	13.3	8.9	8.3	14.3	13.3
P_{loss} (kW)	26.1	29.4	21.6	24.1	26.9	30.0	21.9	24.5	27.1	30.5	22.4	24.7

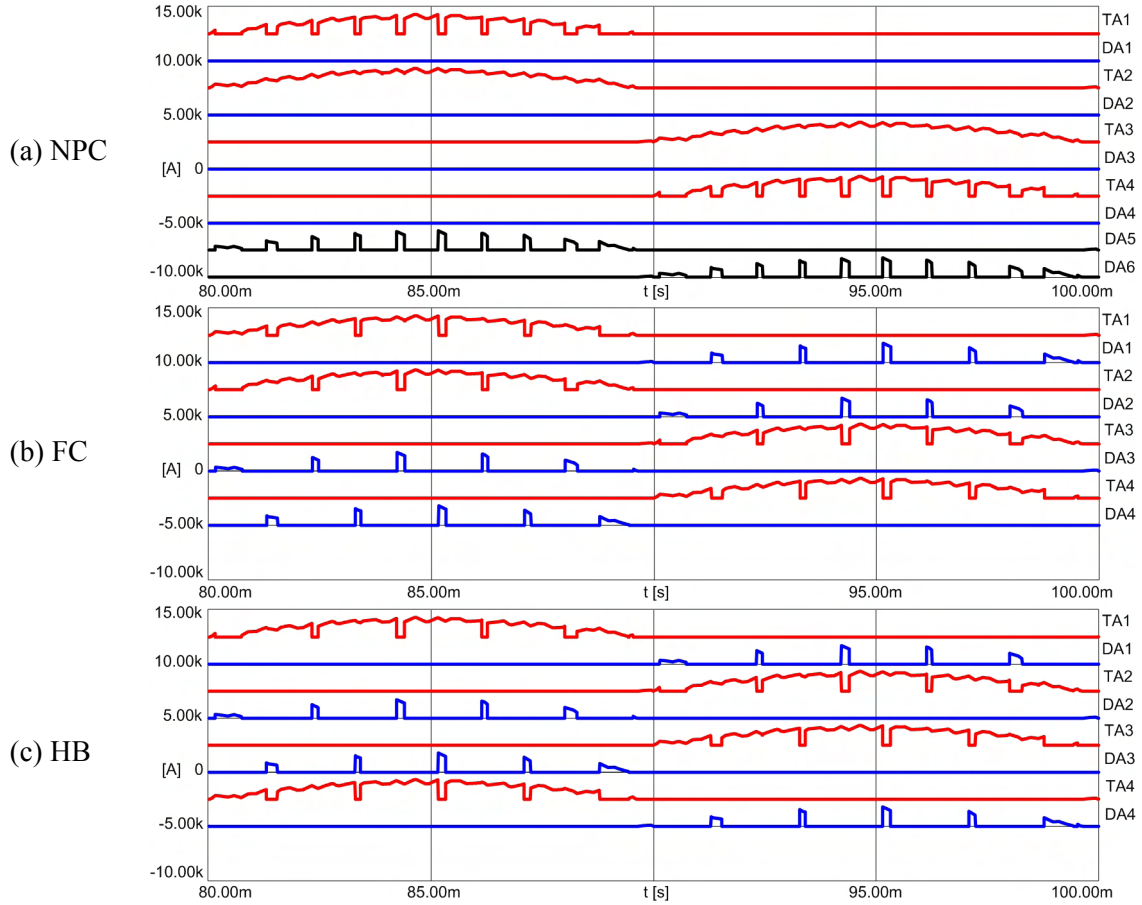

Fig. 7: For f_S=1050Hz & PF=1; IGBT (red), antiparallel diode (blue), and neutral point clamping diode (black) current waveforms with 2500A offsets for phase-a of the NPC (a), the FC (b), and the HB (c) VSCs

Discussions of Power Density and Reliability

Having the identical output performance under the given circuit topologies as obtained by the simulations, power density and reliability for 3L-NPC-, -FC-, and -HB-VSCs are mainly dependent on the aforementioned topological features. Hence, these three converters can be compared in terms of power density and reliability as follows (Table III).

Regarding power density, the FC is expected to be the largest volume due to its flying capacitors. In the NPC, its 3L converter structure with clamping diodes is a volume increasing factor. Moreover, the NPC is expected to require a bigger cooling system than the others if the cooling system for each converter is designed to the keep the most thermally stressed switch (outer IGBTs for the NPC) temperature at the same level in a press-pack switch based converter. Due to the HB's 2L converter structure, the HB is expected to have the less volume than the others. It should be noted that all the

VSCs can use the same filter inductor in the circuit topologies (without capacitive switching ripple filters) considered in this study. Also, the open-winding transformer used for the HB can be assumed to have the same size as the other transformers used for the NPC and FC.

In reliability point of view, flying capacitor lifetime would be a limiting factor for the FC. In the NPC, depending on amount of power loss and thermal characteristics of IGBTs, the higher junction temperature excursion of its outer switches may be a limiting factor compared to the other VSCs. Without three flying capacitors in the FC and without one more DC bus capacitors and eight more clamping diodes, the HB is expected to be more reliable than the others considering this component count advantage. Also, the HB's mature and modular 2L structure with reliable driver and protection schemes is another advantage in practice.

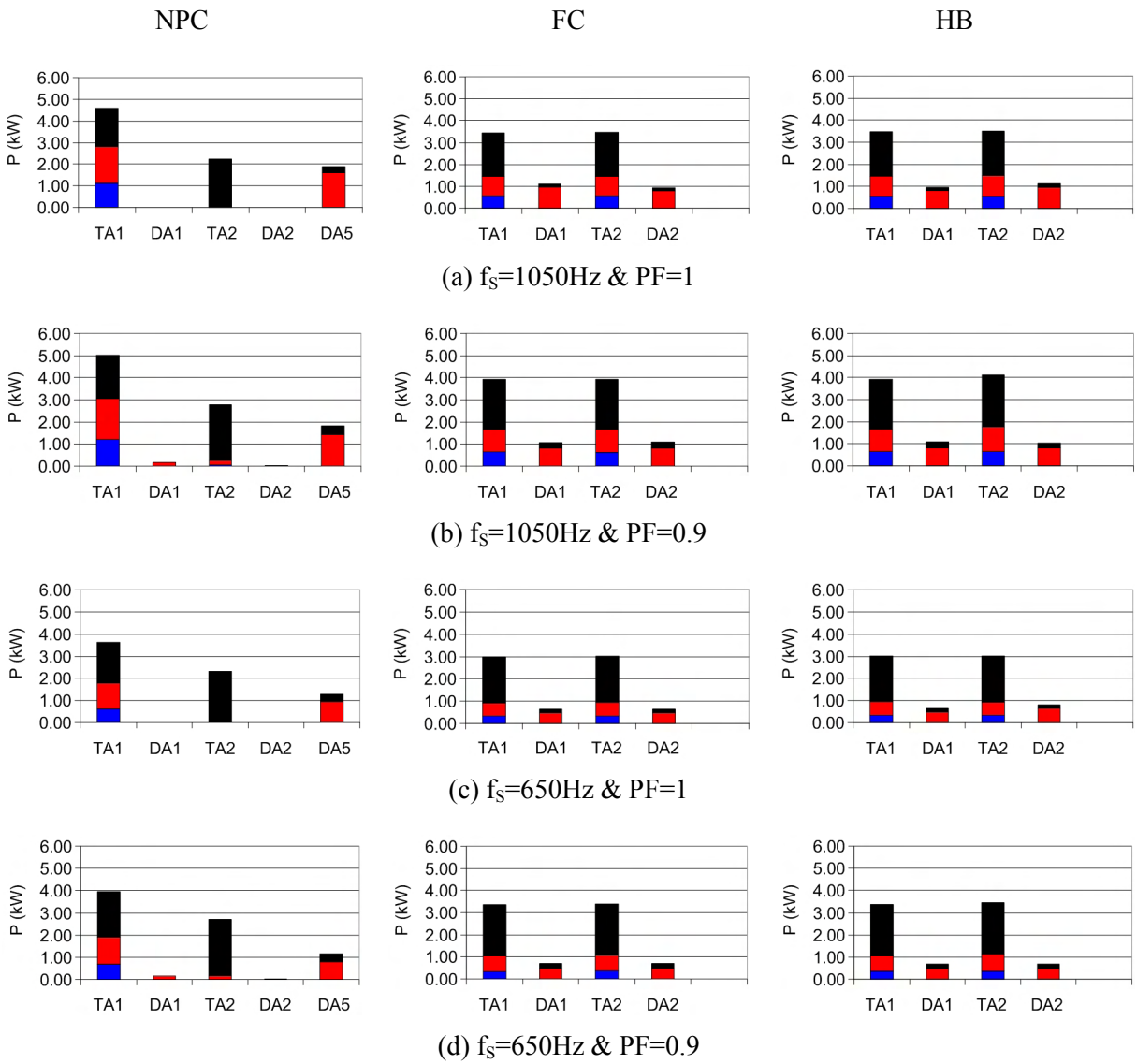

Fig. 8: Turn-on (blue), turn-off/recovery (red), and conduction (black) loss charts for phase-a of the NPC (left), FC (middle), and HB (right) VSCs

Conclusion

This study on the grid connection of a 6MW wind turbine via MV-3L-VSCs shows that the 3L-NPC-, -FC-, and -HB-VSCs are able to produce the same converter outputs with the circuit topologies considered under the operation conditions of f_S and PF. It is observed that the increase of f_S from 650Hz to 1050Hz results in 35% THD_I decrease and in 30% P_{loss} increase. The change of PF from 1 to

0.9 (inductive) results in 10% THD_I decrease and in 12% P_{loss} increase. Unlike THD_I and P_{loss}, the switch utilization differs among the three VSCs such that the NPC results in unbalanced power loss distribution among IGBTs and among diodes whereas the FC and HB distribute the losses more evenly over the converter. In addition to the loss distribution, the topological features of the three VSC favors the HB over the NPC and FC in power density and reliability as generally discussed and summarized in Table III. However, in order to reach more solid conclusions via this comparison, this study and discussion should be extended by considering LCL type switching ripple filters, which are placed between the step-up transformer and the VSC for the grid connection of wind turbines.

Table III: Comparison for power density and reliability

	Power Density	Reliability
3L-NPC	(–) 3L structure with clamping diodes (–) Bigger cooling system than the others due to unbalanced power loss distribution	(–) Higher IGBT junction temperature excursion (–) 6 clamping diodes more than the others
3L-FC	(–) 3 flying capacitors	(–) 3 flying capacitors more than the others
3L-HB	(+) 2L structure (+) Half DC bus capacitance of the others	(+) Mature 2L structure (+) Half the number of DC bus capacitors

References

[1] BTM Consult ApS: World Market Update 2008, Forecast 2009-2013

[2] Grid Code, High and extra high voltage, E.ON Netz GmbH, Bayreuth, Status 1st April 2006

[3] Faulstich A., Steinke J. K., Wittwer F.: Medium voltage converter for permanent magnet generators up to 5 MW, EPE 2005, paper 0145

[4] Andresen B., Birk J.: A high power density converter system for the Gamesa G10x 4.5 MW Wind Turbine, EPE 2007, paper 0185

[5] Wu B.: High-Power Converters and AC Drives, Piscataway, NJ, IEEE Press, 2006, ISBN 978-0-471-731-9

[6] Nabae A., Takahashi I., Akagi H.: A new neutral-point-clamped PWM inverter, IEEE Transactions on Ind. Appl. Vol 1A-17 no 5, pp. 518-523, 1981

[7] Meynard T. A., Foch H., Thomas P., Courault J., Jakob R., Nahrstaedt M.: Multicell converters: basic concepts and industry applications, IEEE Transactions on Ind. Electronics Vol 49 no 5, pp. 955-964, 2002

[8] Tolbert L., Peng F. Z., Habetler T. G.:Multilevel converters for large electric drivers, IEEE Transactions on Ind. Appl. Vol 35 no 1, pp. 36-44, 1999

[9] Rodriguez J., Bernet S., Wu B., Pontt J. O., Kouro S.: Multilevel voltage-source-converter topologies for industrial medium-voltage drives, IEEE Transactions on Ind. Appl. Vol 54 no 6, pp. 2930-2944, 2007

[10] Fazel S. S., Bernet S., Krug D., Jalili K., Design and comparison of 4-kV neutral-point-clamped, flying-capacitor, and series-connected H-bridge multilevel converters, IEEE Transactions on Ind. Appl. Vol 43 no. 4, pp. 1032-1040, 2007

[11] Zeng X., Chen Z., Blaabjerg F., Design and comparison of full-size converters for large variable-speed wind turbines, EPE 2007, paper 0538

[12] Winkelnkemper M., Wildner F., Steimer P.K.: 6 MVA five-level hybrid converter for windpower, PESC 2008

[13] Holmes D. G., Lipo T. A.: Pulse Width Modulation for Power Converters, Piscataway, NJ, IEEE-Wiley, 2003, ISBN 978-0-471-20814-3

[14] Celanovic N., Boroyevich D.: A comprehensive study of neutral-point voltage balancing problem in 3LNPC VS PWM inverters, IEEE Transactions on Power Electronics Vol 15 no 2, pp. 242-249, March 2000

[15] Corzine K.A., Sudhoff S.D., Whitcomb C.A.: Performance characteristics of a cascaded two-level converter, IEEE Transactions on Energy Conversion, Vol 14 no 3, pp.433-439, September 1999

[16] Westcode IGBT T1800GA45A Datasheet

[17] Bruckner T.: The Active NPC Converter for Medium-Voltage Drives, Aachen, Germany, Shaker Verlag, 2006, ISBN 3-8322-5270-3